Journal of Scientific Research & Reports
10(4): 1-8, 2016; Article no.JSRR.24439
ISSN: 2320-0227

SCIENCEDOMAIN *international*
www.sciencedomain.org

Enhanced Performance of a Dye Sensitized Solar Cell Using Silver Nanoparticles Modified Photoanode

Eli Danladi[1*], M. Y. Onimisi[1], S. G. Abdu[2], P. M. Gyuk[2] and Ezeoke Jonathan[1]

[1]Department of Physics, Nigerian Defence Academy, Kaduna, Nigeria.
[2]Department of Physics, Kaduna State University, Kaduna, Nigeria.

Authors' contributions

This work was carried out in collaboration between all authors. Author ED designed the study, undertook the experimental work, performed the statistical analysis, wrote the protocol, wrote the first draft of the manuscript and managed literature searches. Authors MYO, SGA, PMG and EJ managed the analyses of the study and literature searches. All authors read and approved the final manuscript.

Article Information

DOI: 10.9734/JSRR/2016/24439
Editor(s):
(1) Cheng-Fu Yang, Department of Chemical and Materials Engineering, National University of Kaohsiung, Kaohsiung, Taiwan.
(2) Kal Renganathan Sharma, Energy and Manufacturing, Lone Star College, North Harris, USA and Department of Physics, College of Science and Technology, Texas Southern University Houston, TX 77004, USA.
(3) Luigi Rodino, Professor of Mathematical Analysis, Dipartimento di Matematica, Università di Torino, Italy.
Reviewers:
(1) Ong Keat Khim, National Defence University of Malaysia, Malaysia.
(2) Le Anh Tuan, Hanoi University of Science and Technology, Vietnam.
Complete Peer review History: http://sciencedomain.org/review-history/13701

Original Research Article

Received 20th January 2016
Accepted 2nd March 2016
Published 15th March 2016

ABSTRACT

We reported an improved performance of a dye sensitized solar cell (DSSC) using silver nanoparticles (Ag-NPs) modified fluorine tin oxide (FTO) electrode through successive ion layer adsorption and reaction (SILAR). The resulting photoelectrode was successfully incorporated in the DSSC. The photovoltaic performance was evaluated under 100 $mWcm^{-2}$ light intensity. The performance, especially the photocurrent, and open circuit voltage of the DSSC containing Ag-NPs was significantly affected by the Ag-NPs. The modified Ag-NPs photoanode shows a short circuit current density (J_{SC}) of 0.0316 $mAcm^{-2}$, a photovoltage V_{OC} of 0.442 V yielding an overall conversion efficiency of 0.00710%. This represents a 22% improvement in photocurrent over the photocurrent (0.0259 $mAcm^{-2}$) of bare FTO without Ag-NPs.

Keywords: Dye sensitized solar cells; silver nanoparticles; plasmon enhancement.

**Corresponding author: E-mail: danladielibako@gmail.com;*

1. INTRODUCTION

Organic solar cells (OSCs) have the potential to become a promising technology towards the harvesting of solar energy. One of the major advantages that this technology offers is the ability to fabricate devices out of solutions of the active materials employing cheap, scalable printing techniques with low environmental impact [1]. Incorporation of dye molecules in some wide bandgap semiconductor electrodes was a key factor in developing photoelecrochemical solar cells. Michael Gratzel and coworkers at the Ecole Polytechnique Federale de Lausanne [2-4] succeeded for the first time to produce what is known as "Gratzel Cell" or the dye sensitized solar cell (DSSC) to imitate photosynthesis, the natural processes plants convert sunlight into energy by sensitizing a nanocrystalline TiO_2 film using novel ruthenium (Ru) bipyridl complex. In DSSC charge separation is accomplished by kinetics competition like in photosynthesis leading to photovoltaic action. The organic dye monolayer in the photoelectrochemical or DSSC replaces light absorbing pigments (chlorophylls), the wide bandgap nanostructured semiconductor layer replaces oxidized dihydro-nicotinamide-adenine-dinucleotide phosphate (NADPH), and carbon dioxide acts as the electron acceptor. Moreover, the electrolyte replaces the water while oxygen as the electron donor and oxidation product, respectively [5,6]. It has been shown that DSSCs are promising class of low cost and moderate efficiency solar cell based on organic materials [7,8]. DSSCs are based on the photo-injection of electrons from dye molecules into an inorganic semiconductor and holes transport by a redox mediator [9]. The nanoporous structure of the inorganic semiconductor provides the large surface area necessary to achieve significant optical density of the solar cell despite the low light absorption of a dye monolayer [10-12]. However, the porous electrode also plays an important role in the enhancement of recombination processes in the DSSC, thus decreasing all cell parameters and its total conversion efficiency [13-15]. Since the electrolyte penetrates throughout the entire porous structure, a large surface area is available for a reaction between the photo-injected electrons in the semiconductor and the oxidized ions in the redox mediator or oxidized dye at the semiconductor surface [13,16].

Efforts for achieving higher efficiencies are focused in optimizing the morphology of the active photovoltaic layer and the charge transport properties of the absorber through thermal annealing treatment [17,18], use of various solvents [19], the use of additives [20]. Alternatively, introduction of metallic nanoparticles (NPs) in suitable places to trap or confine light inside the active layer and enhance the absorption in the organic semiconductor film could provide superior performances [21-25]. Metal NPs embedded in a dielectric matrix strongly interact with light at their dipole surface plasmon frequency due to the excitation of a collective electron motion (a so called plasmon) inside the metal particle [26]. The surface confines the conduction electrons inside the particle and sets up an effective restoring force leading to resonant behavior at the dipole surface plasmon frequency, namely Surface Plasmon Resonance (SPR). This resonance depends strongly on the shape, size and distribution of the NPs as well as on the dielectric functions of the metal and the dielectric surrounding environment. Therefore, the line-shape of the SPR can be widely tailored. Among the metals that support SPR modes, noble metals, gold, silver and copper (Au, Ag, Cu) exhibit resonances in the visible or near infrared region of the electromagnetic spectrum, which is the range of interest for photovoltaic applications.

Researchers have designed and tested various plasmonic light-trapping geometries for enhancing conversion efficiency of DSSCs [27,28], however, the interaction and working mechanisms in plasmonic DSSCs containing metal nanostructures are dramatically complicated. A detailed description of the kinetics of electrochemical and photoelectrochemical processes in plasmonic DSSCs has not been established [29].

In this present work, Ag-NPs with four SILAR cycles was synthesized on porous TiO_2 film fabricated on FTO substrates. The effects of Ag-NPs on the photovoltaic (PV) performance of the formed DSSC were investigated systematically. The performance characteristics of the plasmonic DSSC were analysed. An overall conversion efficiency of 0.00710% was obtained when Ag-NPs was added, which had a 6% improvement over the performance (0.00670%) of bare FTO based device without Ag-NPs. The related PV performance enhancement mechanisms and surface-plasmon resonances in DSSCs with Ag nanostructures are analysed and discussed.

2. EXPERIMENTAL SECTION

2.1 Synthesis of Nanocomposite Material

Dip coating method was used to synthesize the Ag nanocomposite on the glass substrate. The microscope slide was cleaned with sodium laury sulphate solution and then rinsed with water three times. Thereafter dipped into a beaker containing a mixture of 40 ml concentrated tetraoxosulphate (iv) acid ($H_2SO_{4)}$ and 40 ml chromic acid to make the surface hydrophilic for 10 min, the sample was thereafter rinsed with distilled water. After making it hydrophilic, it was immersed in 2 moles $SnCl_2$ for two (2) min then rinsed with distilled water for 2 min, then immersed in 0.35 mole silver nitrate ($AgNO_3$) for 2 min and rinsed with mixture of 150 ml distilled water (H_2O) and 0.4 moles hydrochloric acid (HCl) for 15 sec. This procedure is called one cycle; the number of cycles was varied upto four cycles to obtain the thickness of the silver deposited.

2.2 Fabrication Process

The FTO electrodes were washed with laury sulphate then later rinsed with water six times in an ultrasonication bath for 10 min, then finally washed in propanol. The photoanode was prepared by first depositing a blocking layer on the FTO glass, followed by the nanocrystalline titanium dioxide (TiO_2.) The blocking layer was deposited from a 2.5 wt% TiO_2 precursor and was applied to the FTO glass substrate by spin coating and subsequently sintered at 450°C for 40 min. The 9 μm thick nanocrystalline TiO_2 layer was deposited by screen printing. It was then sintered in air for 30 mins at 500°C. The silver was deposited on the bare surface of the TiO_2 with four silar cycles that has thickness of 40 nm through successive ion layer adsorption and reaction.

We spin coat titanium tetrachloride ($TiCl_4$) (40 mmoles) at 2500 rpm and thereafter annealed at 200°C to 350°C for 30 min. To ensure the silver was protected, we treated it with 40 mmoles solution of $TiCl_4$ prepared at 40°C, then raised the temperature to 70°C and finally annealed at 300°C to 350°C. Silicon dioxide (SiO_2) was deposited on the Ag using SILAR method with sodium silicate (**Na_2SiO_3**) as the precursor. The minimum number of cycles that gave the cell with Ag-NPs stability was ten cycles. The counter electrode was prepared by screen printing a platinum catalyst gel coating onto the FTO glass. It was then dried at 100°C and fired at 450°C for 30 mins. The method of heating in water was used to extract the dye. Distilled water was the solvent for aqueous extraction. 6 g of the sample (Dried *Hibiscus Sabdariffa* flower) was measured using analytical scale and dipped in 50 ml of the solvent heated to 100°C for 30 min, after which solid residues were filtered out to obtain clear dye solutions. Roselle extract is rich in anthocyanins. It was reported that anthocyanin obtained from roselle are delphinidin and cyanidin complexes [30,31].

The sintered photo anode with four SILAR cycles was sensitized by immersion in the sensitizer solution at room temperature overnight. The cell was assembled by pressing the photoanode against the platinum-coated counter electrode slightly offset to each other to enable electrical connection to the conductive side of the electrodes. Between the electrodes, a 50 μm space was retained using two layers of a thermostat hot melt sealing foil. Sealing was done by keeping the structure in a hot-pressed at 100°C for 1 min. The liquid electrolyte constituted by 50 mmol of iodide/tri-iodide in acetonitrile was introduced by injection into the cell gap through a channel previously fabricated at opposite sides of the hot melt adhesive, the channel was then sealed with an epoxy based two part resin.

2.3 Characterization

The current-voltage (*I-V*) data was obtained using a keithley 2400 source meter under AM1.5 (100 mw/cm^2) illumination from a Newport A solar simulator. Scanning electron micrographs were taken with Phenom Pro X model, Eindhoven de Netherlands SEM. The absorption spectrum of the dye was recorded on Ava-spec-2048 spectrophotometer. The cell active area was 1.82 cm^2. Thickness measurement was obtained with a Dektac 150 surface profiler. X-ray microanalysis was carried out with INCA EDX analyzer. Sheet resistance was obtained with a signatone four point probe resistivity apparatus.

3. RESULTS AND DISCUSSION

Fig. 1 shows the absorbance of the dye and prepared Ag-NPs suspension with the dye within the wavelength range of 350-1000 nm. The absorption peak of *Hibiscus Sabdariffa* dye was observed around 550 nm (indicated in Fig. 1a). The relatively broad and strong enhancement is observed in the range of 370–650 nm with peaks

at about 390 nm and 550 nm as shown in Fig. 1b. (FTO/TiO_2/NPs-Ag) which coincides with the localized surface plasmon resonance (LSPR) band position of decorated Ag-NPs and a peak around 550 nm as shown in Fig. 1b. (FTO/TiO_2). This enhanced absorption and broadened spectrum absorption range of the photoanode was mainly attributed to the SPR of Ag-NPs, which interacted with the dye, enhancing dye absorption that resulted in more charge carrier generation [32].

Fig. 3 shows SEM images of FTO/TiO_2 and FTO/TiO_2/Ag-NPs. The SEM micrograph shows that the TiO_2 nanoparticles produced have a mean particle size of about 25 nm. It also reveals that the surface is porous and has agglomeration.

Fig. 4 shows the X-ray microanalysis of TiO_2. The elements present in the TiO_2 are Titania, Oxygen and Nitrogen. Nitrogen is present due to the blower that was used to dry the TiO_2 semiconductor.

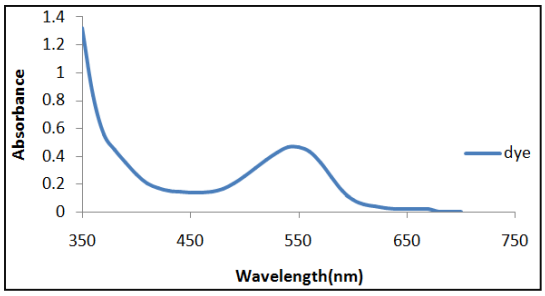

Fig. 1a. UV-vis spectra of the dye

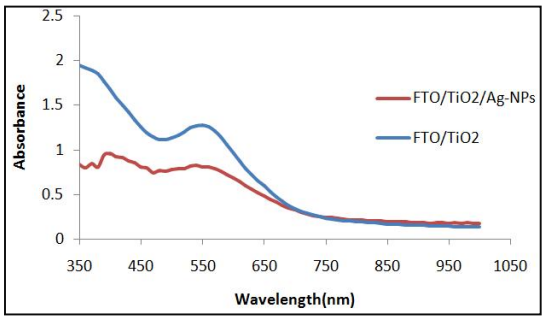

Fig. 1b. UV-vis spectra of FTO/TiO_2, and FTO/TiO_2/Ag-NPs with dye

The absorption of the entire visible region for the electrodes with Ag-NPs was stronger than that for the electrodes without Ag-NPs, which was the product of two distinct effects. First, an absorption attributed to the surface plasmon resonance (SPR) of metallic silver nanoparticles in the TiO_2, [33]. Second, well-separated Ag-NPs with wide range of size and shape exhibits a broad and redshifted SP band, improving the absorption throughout the entire region [34]. Fig. 2 shows the photocurrent density–voltage (*J –V*) curves of the DSSCs with and without silver nanoparticles. Based on the curves in Fig. 2, the *fill factor* (FF) and solar cell efficiency (η) were determined following the equations:

$$FF = \frac{P_{\max}}{P_{in}} = \frac{J_{\max} \times V_{\max}}{J_{SC} \times V_{OC}} \quad (1)$$

$$\eta = \frac{FF \times J_{SC} \times V_{OC}}{P_{IRRADUANCE}}.100\% \quad (2)$$

Where V_{max} = maximum voltage (V);
J_{max} = maximum current density (mA/cm^2);
J_{sc} = short circuit current density (mA/cm^2);
V_{oc} = *open circuit voltage* (V) and
$P_{IRRADIANCE}$ = light intensity (mW/cm^2)

The open-circuit voltage (V_{oc}), short-circuit current density (*Jsc*), fill factor (*FF*), and overall conversion efficiency (η) are summarized in Table 1. The performance of DSSC fabricated with anode deposited on bare FTO substrates was provided for comparison in the Table 1.

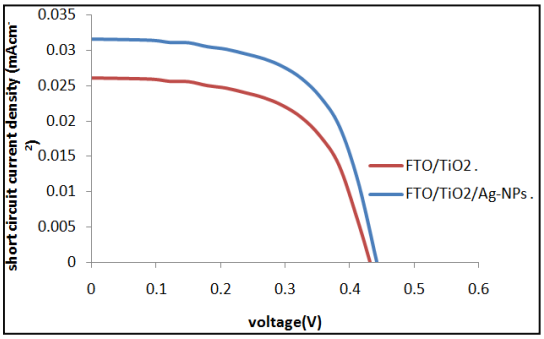

Fig. 2. The photocurrent density–voltage (J –V) curves with and without Ag-NPs

Table 1. Performance characteristics of DSSCs fabricated with different anodes under 100 mWcm^{-2}

Sample	J_{sc} (mAcm^{-2})	V_{oc}(V)	*FF*	η (%)
FTO/TiO_2	0.0259	0.432	0.594	0.00670
FTO/TiO_2/AgNPs	0.0316	0.442	0.507	0.00710

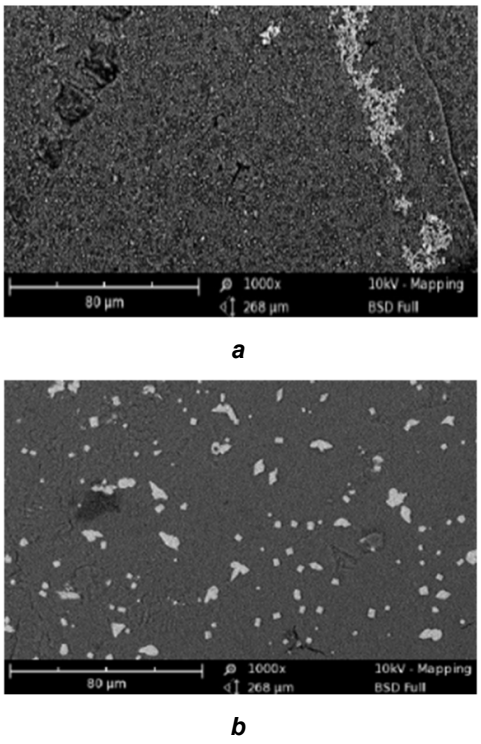

Fig. 3. SEM images of (a) FTO/TiO_2 and (b) FTO/TiO_2/Ag-NPs

The total photon-to-current energy conversion efficiency, for the standard and FTO/TiO_2/Ag-NPs electrodes are 0.0067, and 0.0071%, respectively. The short-circuit photocurrent (*Jsc*) of the electrode with Ag-NPs that was coated upon mesoporous titania was 0.0316 mA/cm^2, an improvement from 0.0259 mA/cm^2 for the pure TiO_2 electrode, exhibiting a 22% enhancement in the charge-separation transfer efficiency. These results were close to those reported previously that revealed plasmon induced enhancement of molecular charge separation [35]. We suggest that the enhanced photocurrent response was mainly attributed to plasmonic scattering which caused an apparent increase of the optical absorption of dye, resulting in a drastically enhanced photocurrent (Fig. 2). The optimum photovoltage may be explained by the fact that, if the Ag nanoparticles and titania are linked together, this leads to shifting conduction band edge of titania negative [36], further increasing the gap between the Fermi level of the photoelectrode and the redox potential under illumination which is the definition of photovoltage [37].

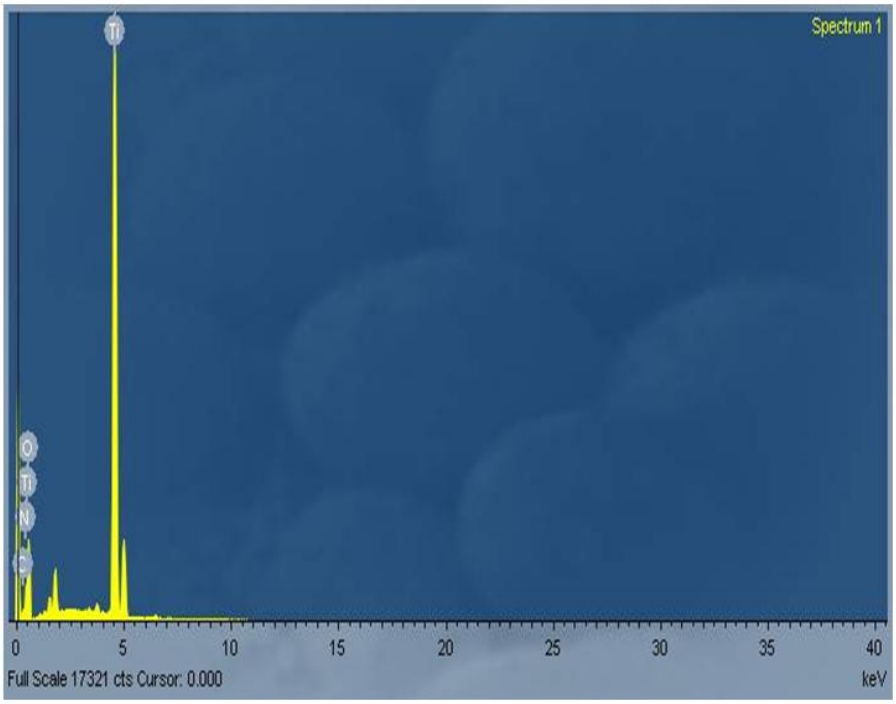

Fig. 4. EDX image showing the elements present in the TiO_2 compound

4. CONCLUSIONS

A TiO_2 photoanodes with an amount of Ag-NPs was investigated through successive ion layer adsorption and reaction. The performance of the DSSC highly depends on the Ag nanoparticles. The results shows that adding Ag-NPs to TiO_2 photoanode significantly improved the performance of the DSSC. The FTO/TiO_2/Ag-NP electrode presents an enhanced photocurrent response compared to the standard electrode. The DSSC containing four SILAR cycles of Ag-NPs, gave a short-circuit current density (J_{sc}) of 0.0316 $mAcm^{-2}$, open-circuit voltage (V_{oc}) of 0.442 V and fill factor (*FF*) of 0.51, yielding an efficiency (η) of 0.00710%. The cell exhibited a 22% improvement over the photocurrent (0.0259 $mAcm^{-2}$) of bare FTO-based device lacking Ag. The increase of J_{SC} is attributed to the enhanced light absorption and broadened absorption spectral range of the composite photoanode due to the Surface Plasmon Resonance of the Ag-NPs, While the *Voc* increase may be reasonably related to the more negative quasi-Fermi energy of the Ag-TiO_2 composite system due to the enhanced electron capture and storage capability resulting from Ag-NP doping.

ACKNOWLEDGEMENTS

The authors are grateful to the physics advanced laboratory, Sheda Science and Technology Complex (SHESTCO), Abuja, Nigeria for the use of their research facilities.

COMPETING INTERESTS

Authors have declared that no competing interests exist.

REFERENCES

1. Nielsen TD, Cruickshank C, Foged S, Thorsen J, Krebs FC. Business, market and intellectual property analysis of polymer solar cells. Solar Energy Materials and Solar Cells. 2010;94:1553–1571.
2. Espinosa N, Garcıa-Valverde R, Urbina A, Krebs FC. A life cycle analysis of polymer solar cell modules prepared using roll-to-roll methods under ambient conditions. Solar Energy Materials and Solar Cells. 2011;95:1293–1302.
3. Gratzel M. Dye-sensitized solar cells. Journal of Photochemistry and Photobiology C: Photochemistry Reviews. 2003;4:145–153.
4. Nazerruddin MK, Kay A, Ridicio I, Humphry-Baker R, Mueller E, Liska P, Vlachopoulos N, Gratzel M. Conversion of light to electricity by cis-X2bis(2,2′-bipyridyl-4,4′-dicarboxylate) ruthenium(II) charge-transfer sensitizers (X = Cl^-, Br^-, I^-, CN^-, and SCN^-) on nanocrystalline TiO_2 electrodes. J. Amer. Chem. Soc. 1993;115: 6382-6390.
5. O'Regan B, Gratzel M. A low cost, high-efficiency solar cell based on dyesensitized colloidal TiO_2 films. Nature. 1991;353: 737–739.
6. Lagref JJ, Nazeeruddin MK, Graetzel M. Artificial photosynthesis based on dye-sensitized nanocrystalline TiO_2 solar cells. Inorganica Chimica Acta. 2008;361(3): 735-745.
7. Smestad GP, Gratzel M. Demonstrating electron transfer and nanotechnology: A natural dye-sensitized nanocrystalline energy converter. Journal of Chemical Education. 1998;75(6):752-756.
8. Hara K, Arakawa H. Dye-sensitized solar cells, In: Handbook of photovoltaic science and engineering, Luque A, Hegedus S, (Ed.), John Wiley & Sons, Ltd. 2003; Chapter 15:663-700.
ISBN: 0-471-49196-9.
9. Hagfeldt A, Gratzel M. Light-induced redox reactions in nanocrystalline systems. Chem. Rev. 1995;95(1):49-68.
10. Parkinson BA, Spitler MT. Recent advances in high quantum yield dye sensitization of semiconductor electrodes. Electrochimica Acta. 1992;37(5):943-948.
11. Argazzi R, Bignozzi CA, Heimer TA, Meyer GJ. Remote interfacial electron transfer from a supramolecular sensitizer. Inorg. Chem. 1997;36:2.
12. Bonhote P, Moser JE, Vlachopoulos N, Walder L, Zakirud-din SM, Humphry-Baker R, Pechy P, Gratzel M. Perfomance of nano structured dye-sensitized solar cell. Chem. Commun. 1996;10.
13. Hagfeldt SE, Lindquist M Gratzel. Mesoscopic solar cells for electricity and hydrogen generation. Sol. Energy Mater. Sol. Cells. 1994;32:245-252.
14. Zaban A Meier, Gregg BA. Electric potential distribution and short range screening in nanoporous TiO_2 electrodes.

J. Phys. Chem. B. 1997;101(40):7985-7990.
15. Bisquert J, Garcia-Belmonte G, Fabregat-Santiago F. Modelling the electric potential distribution in the dark in nanoporous semiconductor electrodes. J. Solid State Electrochem. 1999;3:337-347.
16. Tachibana Y, Moser JE, Gratzel M, Klug D, Durrant JR. Interfacial electron transfer in dye sensitized TiO_2 photoelectrochemical solar cells. J. Phys. Chem in Press. 1996;100.
17. Ma W, Yang C, Gong X, Lee K, Heeger AJ. Thermally stable, efficient polymer solar cells with nanoscale control of the interpenetrating network morphology. Advanced Functional Materials. 2005;15: 1617–1622.
18. Li G, Shrotriya V, Yao Y, Yang Y. Investigation of annealing effects and film thickness dependence of polymer solar cells based on poly(3-hexylthio-phene). Journal of Applied Physics. 2005;98: 043704-1–043704-5.
19. Dang MT, Wantz G, Bejbouji H, Urien M, Dautel OJ, Vignau L, Hirsch L. Polymeric solar cells based on P3HT: PCBM: Role of the casting solvent. Solar Energy Materials and Solar Cells. 2011;95:3408–3418.
20. Lee JK, Ma WL, Brabec CJ, Yuen J, Moon JS, Kim JY, Lee K, Bazan GC, Heeger AJ. Processing additives for improved efficiency from bulk hetero-junction solar cells. Journal of the American Chemical Society. 2008;130: 3619–3623.
21. Westphalen M, Kreibig U, Rostalski J, Luth H, Meissner D. Metal cluster enhanced organic solar cells. Solar Energy Materials and Solar Cells. 2000;61:97–105.
22. Agglund CH, Ach MZ, Kasemo B. Enhanced charge carrier generation in dye sensitized solar cells by nanoparticle plasmons. Applied Physics Letters. 2008; 92:013113-1–013113-3.
23. Stenzel O, Stendal A, Voigtsberger K, Vonborczyskowski C. Enhancement of the photovoltaic conversion efficiency of copper phthalocyanine thin-film devices by incorporation of metal-clusters. Solar Energy Materials and Solar Cells. 1995;37: 337–348.
24. Chen X, Zhao C, Rothberg L. M–KNg plasmon enhancement of bulk heterojunction organic photovoltaic devices by electrode modification. Applied Physics Letters. 2008;93:123302-1–123302-3.
25. Zhu J, Xue M, Shen H, Wu Z, Kim S, Ho JJ, Hassani-Afshar A, Zeng B, Wang KL. Plasmonic effects for light concentration inorganic photovoltaic thin films induced by hexagonal periodic metallic nanospheres. Applied Physics Letters. 2011;98:151110-1–151110-3.
26. Kreibig U, Vollmer M. Optical properties of metal clusters. Springer, Berlin. 1994;77–88.
27. Cole JR, Halas NJ. Optimized plasmonic nanoparticle distributions for solar spectrum harvesting. Applied Physics Letters. 2006;89:153120-1–153120-3.
28. Lagos N, Sigalas MM, Lidorikis E. Theory of plasmonic near-field enhanced absorption in solar cells. Applied Physics Letters. 2011;99:063304-1– 063304-3.
29. Dingwen Zhang, Milton Wang, Alexandre G. Brolo, Jie Shen, Xiaodong Li, Sumei Huang. Enhanced performance of dye-sensitized solar cells using gold nanoparticles modified fluorine tin oxide electrodes. J. Phys. D: Appl. Phys. 2013;46:024005:8.
30. Frank T, Clin J. The effect of St John's wort extracts on CYP3A: A systematic review of prospective clinical trials. Pharmacol. 2005;45:203.
31. Terahara N, Saito N, Honda T, Tokis K, Osajima Y. Acylated anthocyanins of *Clitoria ternatea* flowers their acyl moieties. Phytochemistry. 1990;29:949.
32. Kaimo Guo, Meiya Li, Xiaoli Fang, Xiaolian Liu, Bobby Sebo, Yongdan Zhu, Zhongqiang Hu, Xingzhong Zhao. Preparation and enhanced properties of dye-sensitized solar cells by surface plasmon resonance of Ag nanoparticles in nanocomposite photoanode. Journal of Power Sources. 2013;230:155-160.
33. Wang H, Kim DY, Choi KW, Seo JH, Im SH, Park JH, Park OO, Heeger AJ. Enhancement of donor-acceptor polymer bulk heterojunction solar cell power conversion efficiencies by addition of Au nanoparticles. Angewandte Chemie International Edition. 2011;50:5519–5523.
34. Matsubara K, Tatsuma T. Morphological changes and multicolor photochromism of Ag nanoparticles deposited on single-crystalline TiO_2 surfaces. Adv. Mater. 2007;19:2802–2806.
35. Su-Jien Lin, Kuang-Che Lee, Jyun-Lin Wu, Jun-Yi Wu. Plasmon- enhanced photocurrent in dye-sensitized solar cells. Solar Energy. 2012;86:2600–2605.

36. Jakob M, Levanon H, Kamat PV. Charge distribution between UV-irradiated TiO_2 and gold nanoparticles: Determination of shift in the Fermi level. Nano Lett. 2003;3: 353–358.

37. Martinson ABF, Hamann TW, Pellin MJ, et al. New architectures for dye-sensitized solar cells. Chem. – Eur. J. 2008;14: 4458–4467.

Peer-review history:
The peer review history for this paper can be accessed here:
http://sciencedomain.org/review-history/13701